Materials Science-Poland, *Vol. 28*, *No. 4*, *2010*

Cycling behaviour of barium doped $LiMn_2O_4$ cathode materials for Li ion secondary batteries

H. SAHAN*, H. GÖKTEPE, S. PATAT

Department of Chemistry, Faculty of Science, Erciyes University, 38039 Kayseri, Turkey

In order to improve the cycling performance of $LiMn_2O_4$, the spinel phase $LiMn_{2-x}Ba_xO_4$ (x = 0.01, 0.02 and 0.05) compounds were fabricated by the glycine-nitrate method. The structures of the products were investigated by X-ray diffraction. Electrochemical studies were carried out using the Li|$LiMn_2O_4$ and Li|$LiMn_{2-x}Ba_xO_4$ cells. The capacity loss of Li|$LiMn_2O_4$ cell is about 15% after 30 cycles, whereas that for Ba doped spinel materials (x = 0.01, 0.02 and 0.05) are 7.5%, 3.5% and 1.8% respectively. The good capacity retention of $LiMn_{2-x}Ba_xO_4$ electrodes is attributed to stabilization of the spinel structure by Ba doping of Mn sites. Ba substituted spinels display better cycle performance in terms of cycle life compared with $LiMn_2O_4$.

Keywords: *$LiMn_2O_4$; glycine nitrate method; cycle life; Ba doping*

1. Introduction

Increasing demand for portable electronic devices is driving the development of compact lightweight batteries of high energy density. Lithium secondary batteries show great promise as power sources for portable electronic devices such as cellular phones, camcorders and laptop computers because of their high output voltages, high specific energy densities, and excellent cycle performance [1]. Among the cathodic materials investigated, $LiMn_2O_4$ based spinels are promising candidates for replacing $LiCoO_2$, which is the material currently used in commercial lithium batteries. Spinel $LiMn_2O_4$ has been considered a potential alternative to $LiCoO_2$ for use as the positive electrode in rechargeable lithium ion batteries because of its low cost, environmental friendliness and high safety [2–4]. However, stoichiometric $LiMn_2O_4$ exhibits an unacceptably high capacity fade on cycling. The origin for this capacity loss has not been clearly identified, but several possibilities exist, e.g. (i) occurrence of lattice (Jahn–Teller) distortion on the surface of $LiMn_2O_4$ due to inhomogeneity in discharge and formation of tetragonal $Li_2Mn_2O_4$ [5],(ii) manganese dissolution into electrolyte [6],

*Corresponding author, e-mail: halil@erciyes.edu.tr

(iii) formation of oxygen defects [7], (iv) formation of new phases [8], (v) loss of crystallinity [9], (vi) instability arising from the existence of two cubic phases during the charge–discharge process [10].

Among various approaches to overcome these problems, one effective approach is to substitute a small amount of Mn ions with dopant ions [11, 12]. It is believed that the dopant ions occupy 16d sites of Mn ions in the spinel lattice and stabilize the spinel structure. Research shows that suitable elements doping are good way of improving the properties of $LiMn_2O_4$ cathode materials [13]. Extensive research studies on doping have hitherto focused on such elements as Na, Mg, Al, Zn, B, F, S, Co, Ti, Cr, Mn, Cd, Sn, Ga, Fe, etc. [14–17]. However, the atomic radii of all these elements are lower than or comparable to that of Mn.

In this work Ba was selected as the substitute material, because it has a larger atomic radius than Mn. Bare and Ba substituted materials were prepared by the rapid glycine-nitrate method (GNM) and wherein Mn was partially replaced with Ba ions, to improve the cycle performance of $LiMn_2O_4$ spinel materials.

2. Experimental

$LiMn_2O_4$ and $LiMn_{2-x}Ba_xO_4$ (x = 0.01, 0.02 and 0.05) spinels were fabricated with stoichometric amounts of raw $LiNO_3$ (Riedel-de Haen), $Mn(CH_3COO)_2{\cdot}4H_2O$ (Sigma) and $Ba(NO_3)_2$ (Surechem). The raw materials were dissolved in distilled water. Glycine (Merck) was added to the mixture either as a solid or as water solution. Its role was to serve both as a fuel for combustion and as a complexing agent to prevent inhomogeneous precipitation of individual components prior to combustion. Finally, nitric acid with the same concentration of acetate anions was added to the solution. The molar ratio of glycine to nitrate was 1:4. The solution was heated continuously without any previous thermal dehydration. Afterwards the solution became a transparent viscous gel which auto-ignited automatically, giving a voluminous, black, sponge-like ash product of combustion. The resulting ash was heated at 800 °C for 12 h.

Phase identification of the samples was carried out by the XRD analyses using a Bruker AXS D8 diffractometer with monochromatic CuK_α radiation. The DiffracPlus and Win-Metric programs were used to obtain information about the crystal structures of the samples. In all cases, the XRD patterns could be indexed based on a cubic cell. The morphologies of the powders were observed using a scanning electron microscope (SEM, LEO 440) operated at 20 kV.

Electrochemical studies were performed using a cylindrical two-electrode teflon cell assembled in an argon-filled dry box and tested at room temperature. Fabrication of the electrodes was as follows. The cathode material consisted of 86 wt. % of active material, 9 wt. % of acetylene black was used as the conductive material and 5 wt. % of poly(tetrafluoroethylene) as a binder. A lithium piece 13 mm in diameter, 1 M $LiPF_6$ solution in ethylene carbonate/diethyl carbonate (EC:DEC = 1:1) and a glass filter were used as the anode, electrolyte and separator, respectively.

Diethyl carbonate, ethylene carbonate, and acetylene black were used after purification by the methods described elsewhere [18]. 100 cm^3 of diethyl carbonate (DEC) was washed with aqueous 10% Na_2CO_3 solution (20 cm^3), saturated $CaCl_2$ (20 cm^3) and then with water (30 cm^3). After drying over solid $CaCl_2$ for 1 h (note that prolonged contact should be avoided because slow combination with $CaCl_2$ occurs), it should be fractionally distilled. Ethylene carbonate was dried over P_2O_5, then fractionally distilled under the pressure of 10 mm Hg and crystallized from dry ethyl ether. Acetylene black was leached for 24 h with 1:1 HCl to remove oil contamination, then washed repeatedly with distilled water. Then it was dried in air, and eluted for 1 day each with benzene and acetone. Again it was dried in air at room temperature and then heated in vacuum for 24 h at 600 °C to remove adsorbed gases.

The test cell performance was measured on a computer controlled multi-channel charge/discharge apparatus (MLab100, Wenking). In order to study their cycling performance, the test cells were galvanostatically charged/discharged at a constant current rate of 1 C within the voltage range of between 3.5 V and 4.5 V (vs. Li/Li^+).

3. Results and discussion

The powder X-ray diffraction patterns of the $LiMn_2O_4$ and $LiMn_{2-x}Ba_xO_4$ (x = 0.01, 0.02 and 0.05) are shown in Fig. 1. The XRD spectra confirmed there were no phase differences between the Ba doped $LiMn_2O_4$ spinel samples and pure, undoped $LiMn_2O_4$ spinel samples (in particular, BaO phase was not present in the Ba doped $LiMn_2O_4$ samples).

The powder X-ray diffraction patterns of the samples synthesised for this study could be indexed to the spinel space group (*Fd*3*m*) in which lithium ions occupy the tetrahedral (8a) sites. Mn^{3+} and Mn^{4+} ions as well as the doping metal ions, as in $LiMn_2O_4$ structure, occupy the (16d) sites [19]. For simplicity, these structures can be expressed as $[Li]_{tetrahedral}[Mn_{2-y}M_y]_{octahedral}[O_4]$ [20]. The ionic radius of six coordinate Mn^{4+} is 0.53 Å, but the ionic radius of six coordinate Mn^{3+} depends on the spin state. In the low spin state (LS) its ionic radius is 0.58 Å, but in the high spin state (HS) it is 0.645 Å. However, the ionic radius of sixth coordinate Ba^{2+} is 1.49 Å [21]. Therefore, the lattice parameter of substituted spinel should be higher than that of undoped spinel $LiMn_2O_4$.

Table 1. The cubic lattice parameter a and the unit cell volume V for $LiMn_2O_4$ and $LiMn_{2-x}Ba_xO_4$ (x = 0.01, 0.02 and 0.05) samples

Compound	a [Å]	V [$Å^3$]
$LiMn_2O_4$	8.24095 ± 0.00163	559.669
$LiMn_{1.99}Ba_{0.01}O_4$	8.24150 ± 0.00272	559.781
$LiMn_{1.98}Ba_{0.02}O_4$	8.23597 ± 0.00163	558.656
$LiMn_{1.95}Ba_{0.05}O_4$	8.23846 ± 0.00163	559.162

On the contrary, as shown in Table 1, the cubic lattice parameters of Ba substituted spinels, as calculated with the Win-Metric program, were similar or lower than those of the unsubstituted compound. This may be explained by the fact that the value of $\Delta_f G$ of BaO (–525 kJ·mol^{-1}) is more negative than $\Delta_f G$ of MnO_2 (–465 kJ·mol^{-1}). Thus, doped metal ions enhance the stability of the octahedral sites and decrease the lattice constant of a spinel skeleton structure because the bonding energy of the doped metal oxygen (Ba–O: 548 kJ·mol^{-1}) is stronger than that of Mn–O (402 kJ· mol^{-1}) [22]. A similar result was also reported by Xu et al. [23].

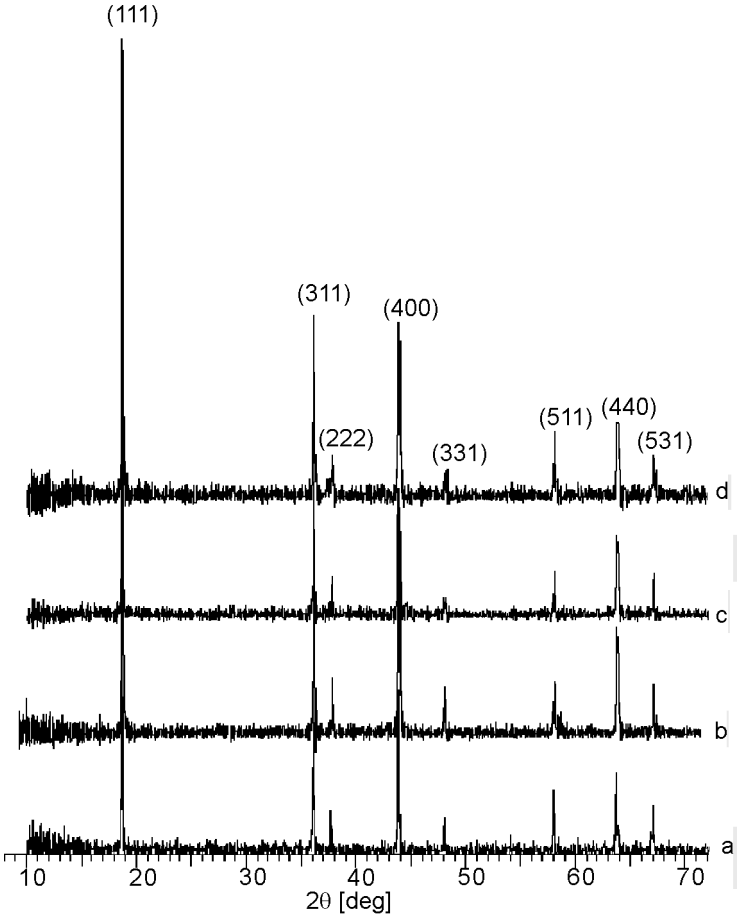

Fig. 1. X-ray diffraction patterns of: a) $LiMn_2O_4$, b) $LiMn_{1.99}Ba_{0.01}O_4$, c) $LiMn_{1.98}Ba_{0.02}O_4$, d) $LiMn_{1.95}Ba_{0.05}O_4$ powders

Because the particle size and surface morphology are also important factors for the cycling performance of cathode materials, they were examined by SEM. Figure 2 shows the micrographs of $LiMn_2O_4$ and $LiMn_{2-x}Ba_xO_4$ (x = 0.01, 0.02 and 0.05) powders. The average particle size of all samples was calculated by the Image Pro-Plus 5.0

program. The average particle sizes of the powders were slightly below 400 nm. The substituted spinel particles are not isolated, but are connected (cf. Figs. 2a–d). Consequently, the specific surface area of substituted spinel particles decreases. Matsuda et. al reported that the smaller the specific surface area of active material particles, the better the cycle performance of the cell is [24]. Thus we may expect the capacity fade of the Li|$LiMn_{2-x}Ba_xO_4$ (x = 0.01, 0.02 and 0.05) cell to be lower than that of the Li|$LiMn_2O_4$ cell; large specific surface area of $LiMn_2O_4$ particles promotes Mn dissolution into the electrolyte.

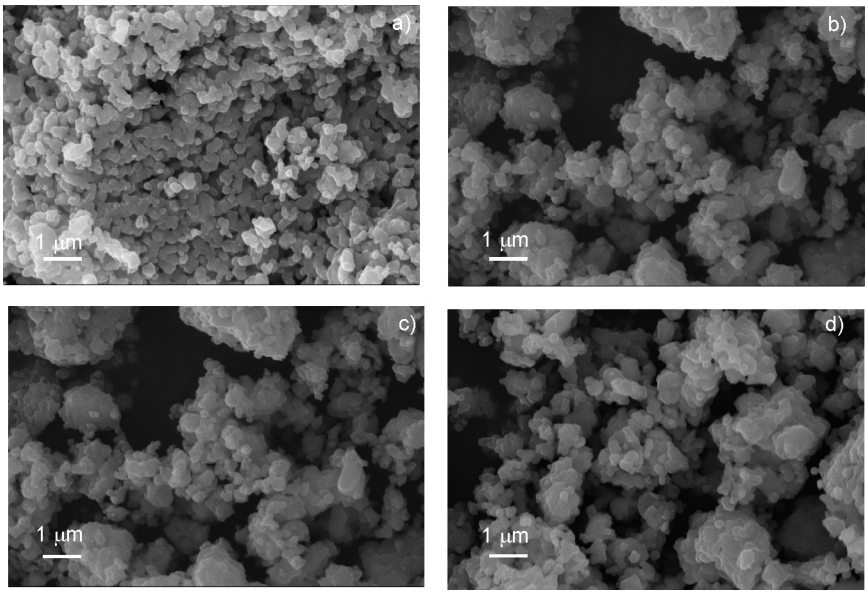

Fig. 2. Scanning electron micrographs of spinel powders:
$LiMn_2O_4$ (a), $LiMn_{2-x}Ba_xO_4$, x = 0.01 (b), x = 0.02 (c) and x = 0.05 (d)

Figure 3 shows the discharge profiles of $LiMn_2O_4$ and $LiMn_{2-x}Ba_xO_4$ (x = 0.01, 0.02 and 0.05) cathodes for 1–30th cycles at room temperature. As can be clearly seen, the discharge curves of all samples had two plateaus at approximately 4.0 and 4.1 V, which indicates a remarkable characteristic of a well defined $LiMn_2O_4$ spinel. The initial discharge capacity of the Li|$LiMn_2O_4$, Li|$LiMn_{2-x}Ba_xO_4$ (x = 0.01, 0.02 and 0.05) cells reached 120.1, 115.2, 115.2 and 89.7 mAh·g^{-1}, respectively. This is due to the decreasing amount of Mn^{3+} ions in the substituted spinel phase, since during the intercalation–deintercalation of Li^+ in $LiMn_2O_4$ only the Mn^{3+} contributes to the charge capacity.

Dependences of the discharge capacity on the cycle number for all cathodes are shown in Fig. 4. The discharge capacity and capacity fading rates for various numbers of cycles were evaluated (Table 2). As is clearly seen, the cycle performance of the Ba doped $LiMn_2O_4$ cathodes was a significant improvement over the undoped cathodes. After 30 cycles, the discharge capacity and capacity loss of undoped $LiMn_2O_4$ was

101.7 mAh·g^{-1} and 15.1%, respectively. However, the discharge capacity of $LiBa_{0.02}Mn_{1.98}O_4$ still kept 111.2 mAh·g^{-1} and capacity fading was only 3.5%, after 30 cycles. As shown in Fig. 4 and Table 2, $LiMn_{1.99}Ba_{0.01}O_4$ and $LiMn_{1.98}Ba_{0.02}O_4$ electrodes have the same initial discharge capacity but the discharge capacity fade of the $LiMn_{1.99}Ba_{0.01}O_4$ electrode is higher than that of the $LiMn_{1.98}Ba_{0.02}O_4$ electrode. Although initial discharge capacity fading of $LiMn_{1.95}Ba_{0.05}O_4$ electrode is only 1.8% because the molar ratio of Ba^{2+} ions in the crystal lattice is increased, this electrode has the lowest initial discharge capacity. For these reasons, the electrode performance of $LiMn_{1.98}Ba_{0.02}O_4$ is better than the others.

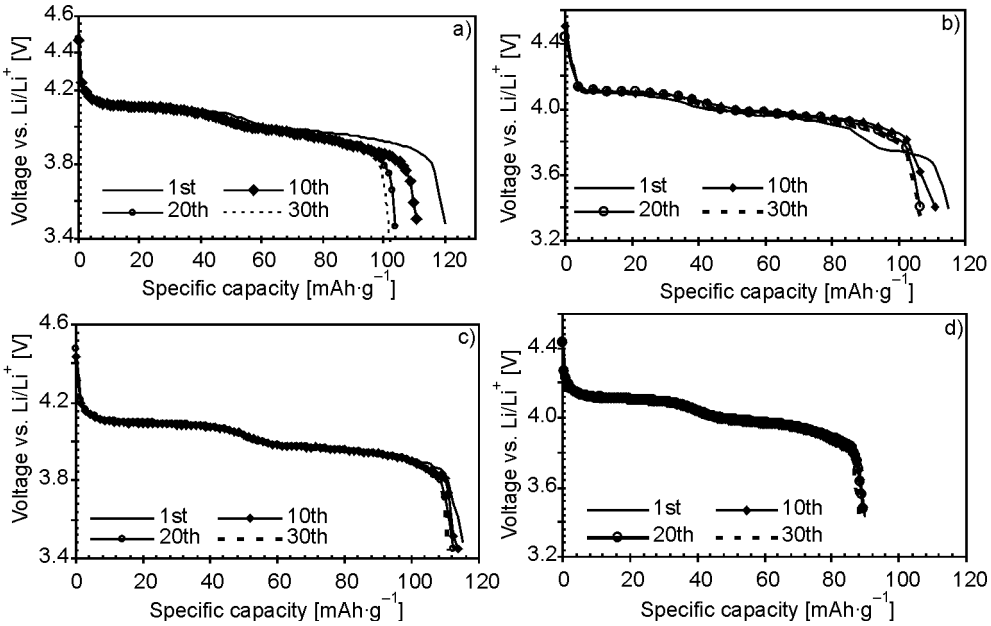

Fig. 3. Discharge profiles of the electrodes: $LiMn_2O_4$ (a) and $LiMn_{2-x}Ba_xO_4$; $x = 0.01$ (b), $x = 0.02$ (c), $x = 0.05$ (d)

Table 2. Discharge capacity performance of the base Li|$LiMn_2O_4$ and Li|$LiMn_{2-x}Ba_xO_4$ ($x = 0.01$, 0.02 and 0.05) cells

Cathode material	Discharge capacity (mAh·g^{-1})				Capacity fading [%]
	1st	10th	20th	30th	
$LiMn_2O_4$	120.1	111.1	104.0	101.7	15.3
$LiMn_{1.99}Ba_{0.01}O_4$	115.2	115.2	111.0	106.6	7.5
$LiMn_{1.98}Ba_{0.02}O_4$	115.2	114.0	112.6	111.2	3.5
$LiMn_{1.95}Ba_{0.05}O_4$	89.7	89.7	89.3	88.1	1.8

Because barium substitutes manganese in the lattice, the decrease of Mn^{3+} reduces the Jahn–Teller distortion and also stabilizes the structural integrity, improved electro-

chemical stability of $LiMn_{2-x}Ba_xO_4$ (x = 0.01, 0.02 and 0.05) electrodes is obtained. In addition, the bonding energy of Ba–O is higher than that of Mn–O. Thus the dopants enhance the stability of the spinel structure and prevent structural degradation of the material.

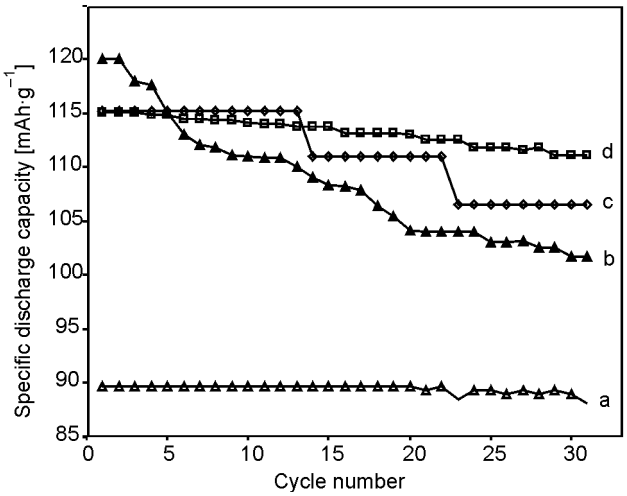

Fig. 4. Dependences of discharge capacity on the cycle number for the cells: Li|$LiMn_2O_4$ (b) and Li|$LiMn_{2-x}Ba_xO_4$; x = 0.01 (c), x = 0.02 (d) and x = 0.05 (a)

As recent work has shown, Er and La doped $LiMn_2O_4$ spinel has excellent cycling performance, and cell polarization decreased as the number of cycles increased [25, 26]. Thus, we assumed that Ba doping improves cathodic properties of $LiMn_2O_4$ and ensures better electrochemical performance.

4. Conclusions

In this study, $LiMn_2O_4$ and $LiMn_{2-x}Ba_xO_4$ (x = 0.01, 0.02 and 0.05) powders having spinel structure were synthesized by the glycine-nitrate method. $LiMn_{2-x}Ba_xO_4$ (x = 0.01, 0.02 and 0.05) cathode materials showed lower initial discharge capacity than unmodified $LiMn_2O_4$. Chemical substitution of Ba for Mn in $LiMn_2O_4$ improves the cycling performance. The improvement in the cycling properties might be attributed to the stabilization of the spinel structure and the suppression of the Jahn–Teller distortion via Ba metal doping. Tu et al. confirmed that the charge transfer resistance is slowed down by La doping on $LiMn_2O_4$ [26]. We may expect that the effect on charge transfer resistance of Ba doping is the same as La doping.

Acknowledgements

This study was financially supported by the Research Foundation of Erciyes University (Kayseri, Turkey). The authors thank Mrs. F.Kılıç for the SEM observation.

References

[1] KIM J., MANHIRAM A., Nature, 390 (1997), 265.
[2] SUN X., YANG X.O., BALASUBRAMANIAN M., MCBREEN J., XIA Y., SAKAI T., J. Electrochem. Soc., 149 (2002), A842.
[3] SAITOH M., SANO M., FUJITA M., SAKATA M., TAKATA M., NISHIBORI E., J. Electrochem. Soc., 151 (2004), A17.
[4] REIMERS J.N., DAHN R.J., J. Electrochem. Soc., 151 (1992), 2091.
[5] THACKERAY M.M., SHAOHORN Y., KAHAIAN A.J., KEPLER K.D., SKINNER E., VAUGHEY T., HACKNEY S.A., Electrochem. Solid State Lett., 1 (1998), 7.
[6] YAMANE H., INOUE T., SANO M., J. Power Sources, 99 (2001), 60.
[7] WANG X., NAKAMURA H., YOSHIO H., J. Power Sources, 110 (2002), 19.
[8] PALACIN M.R., CHABRE Y., DUPONT L., HERVIEU M., MASQUELIER C., J. Electrochem. Soc., 47 (2000), 845.
[9] HUANG H., VINCENT C.A., BRUCE P.G., J. Electrochem. Soc., 146 (1999), 3649.
[10] XIA Y., YOSHIO M., J. Power Sources, 66 (1997), 129.
[11] EIN-ELI Y., VAUGHTY J.T., THACKERAY M.M., MUKERJEE S., YANG X.Q., MCBREEN J., J. Electrochem. Soc., 146 (1999), 908.
[12] HAYASHI N., IKUDA H., WAKIHARA M., J. Electrochem. Soc., 146 (1999), 1351.
[13] HWANG B.J., SANTHANAM R., HU S.G., J. Power Sources, 108 (2002), 250.
[14] FU Y.P., SU Y.H., LI.C.H., Solid State Ionics, 166 (2004), 137.
[15] TANIGUCHI I., Mater. Chem. Phys., 92 (2005), 172.
[16] SAHAN H., GÖKTEPE H., PATAT S., Inorg. Mater., 44 (2008), 420.
[17] LIU R.S., SHEN C.H., Solid State Ionics, 157 (2003), 95.
[18] ARMAREGO W.L.F., PERIN D.D., *Purification of Laboratory Chemicals*, Heinemann, 4th Ed. Oxford, 2002.
[19] GUOHUA L., IKUTA H., UCHIDA T., WAKIHARA M., J. Electrochem. Soc., 143 (1996), 178.
[20] WEST A.R., *Basic Solid State Chemistry*, Wiley, New York, 1991, p. 57.
[21] SHANNON R.D., Acta Cryst., A32 (1976), 751.
[22] BREWER L., BRACKETT E., Chem. Rev., 61 (1961), 425.
[23] XU C.Q., LIU L.Y., Mater. Chem. Phys., 98 (2006), 532.
[24] MATSUDA K., TANIGUCHI I., J. Power Sources, 132 (2004), 156.
[25] LIU H.W., ZHANG K.L., Matter. Lett., 58 (2004), 3049.
[26] TU J., ZHAO X.B., ZHUANG D.G., ZHU T.J., TU J.P., Physica B, (2006), 382.

Received 19 March 2009
Revised 28 October 2010